CHAPTER W20

Thin Films, Interfaces, and Multilayers

W20.1 Strength and Toughness

Having seen how a film adheres to the surface, attention now turns to a study of its mechanical strength. The strength of the bond of a thin film to a substrate may be determined by comparing the surface energies before and after separation. Let $\gamma_{SS'}$ denote the surface tension between the film and the substrate. In delaminating the film from the substrate new solid–vapor interfaces are created, so the change in surface energy per unit area, called the *intrinsic toughness*, is given by the *Dupré formula*:

$$\delta u = \gamma_{SV} + \gamma_{S'V} - \gamma_{SS'}. \tag{W20.1}$$

This is a positive number because it takes energy to create a cleavage.

If sufficient stress is applied to a film in the direction normal to the interface, the film will separate from the surface. The maximum stress the interface can withstand will be denoted by $\sigma_{\max}$. Let $\sigma_{zz}(z)$ denote the stress needed to separate the film a distance z from the equilibrium position, taken to be $z = 0$. Then

$$\delta u = \int_0^\infty \sigma_{zz}(z)\, dz. \tag{W20.2}$$

In the case of metal films on metal substrates, it has been found that the stress may be obtained by taking the derivative of a potential energy per unit area of the empirical form

$$u(z) = F\left(\frac{z}{a}\right) \Delta E, \tag{W20.3}$$

where ΔE and a are parameters that depend on the metals and F is the universal function:

$$F(t) = -(1 + t)e^{-t}. \tag{W20.4}$$

It is believed that this form results from the formation of bond charge at the interface and depends on the exponential falloff of the wavefunctions into vacuum. It is also believed that this formula applies as well to covalent bonds. The stress is therefore

$$\sigma_{zz} = \frac{\Delta E}{a^2} z e^{-z/a}. \tag{W20.5}$$

It rises from zero at the surface, goes through a maximum at $z = a$, and falls off with further increase in z. At the maximum it has the value

$$\sigma_{\max} = \frac{\Delta E}{ae}, \tag{W20.6}$$

where $e = 2.718$. Integrating the analytical formula for the stress results in the expression

$$\sigma_{\max} = \frac{\delta u}{ae} = \frac{\gamma_{SV} + \gamma_{S'V} - \gamma_{SS'}}{ae}. \tag{W20.7}$$

W20.2 Critical Thickness

If a crystalline film grows epitaxially on a substrate in such a way that both are constrained to be flat, there is a critical film thickness beyond which misfit dislocations will develop. This often leads to degradation of the mechanical and electrical properties of the film. The theory of Freund and Nix[†] generalizes earlier work by Matthews and Blakeslee[‡], who analyzed this phenomenon for the case of a thin film on a thick substrate. This critical thickness is determined by the condition that the work needed to produce a dislocation be equal to the strain energy recovered from the system. Letting a_f and a_s be the stress-free lattice constants for the film and substrate, respectively, and ε_f and ε_s be the corresponding strains, one has

$$\varepsilon_m = \frac{a_s - a_f}{a_f} \approx \varepsilon_f - \varepsilon_s \tag{W20.8}$$

for the mismatch strain.

It will be convenient to assume that the film and substrate are both isotropic materials and that they have identical mechanical properties, such as G, the shear modulus, and ν, the Poisson ratio. The film and substrate are subjected to a biaxial stress. The components of the stress tensor may be expressed as $(\sigma_1, \sigma_2, \sigma_3, \sigma_4, \sigma_5, \sigma_6) = (P, P, 0, 0, 0, 0)$, where P is the in-plane pressure. The compliance tensor S_{ij} will be of the same form as Eq. (10.18) in the textbook[§] with S_{ij} elements replacing C_{ij} elements. Using Eq. (10.14*b*), the elements of the strain tensor are $(\varepsilon_1, \varepsilon_2, \varepsilon_3, \varepsilon_4, \varepsilon_5, \varepsilon_6) = (P(S_{11} + S_{12}), P(S_{11} + S_{12}), 2S_{12}P, 0, 0, 0)$. Note that $\varepsilon_1 = \varepsilon_2 = \varepsilon_m$. The *biaxial modulus* M common to both the substrate and the film is defined by the relation $\varepsilon_1 = P/M$. From Table 10.4, using $S_{11} - S_{12} = 1/(2G)$ and $S_{12} = -\nu S_{11}$, one obtains an expression for the biaxial modulus:

$$M = 2G\frac{1 + \nu}{1 - \nu}. \tag{W20.9}$$

[†] L. B. Freund and W. D. Nix, *Appl. Phys. Lett.*, **69**, 173 (1996).

[‡] J. W. Matthews and A. E. Blakeslee, *J. Cryst. Growth*, **27**, 118 (1974).

[§] The material on this home page is supplemental to the *The Physics and Chemistry of Materials* by Joel I. Gersten and Fredrick W. Smith. Cross-references to material herein are prefixed by a "W"; cross-references to material in the textbook appear without the "W."

The net force per unit length on a plane perpendicular to the interface must vanish, so

$$M\varepsilon_f t_f + M\varepsilon_s t_s = 0, \tag{W20.10}$$

where t_f and t_s are the corresponding thicknesses of the film and substrate. Thus

$$\varepsilon_s = -\varepsilon_m \frac{t_f}{t_f + t_s}, \qquad \varepsilon_f = \varepsilon_m \frac{t_s}{t_f + t_s} \tag{W20.11}$$

before any dislocations are generated.

The geometry is illustrated in Fig. W20.1 both before and after the dislocation is formed in the substrate. Let **b** be the Burgers vector of the dislocation, b_x and b_y its components parallel to the interface, and b_z the perpendicular component. From elasticity theory, the long-range attractive force per unit length on the edge dislocation from both free surfaces is estimated to be

$$F(z) = \frac{G[b_x^2 + b_y^2 + (1-\nu)b_z^2]}{4\pi(1-\nu)} \left(\frac{1}{z} - \frac{1}{t_s + t_f - z} \right). \tag{W20.12}$$

The direction of the force is shown in Fig. W20.1. The energy released per unit thickness when the strain in the substrate is relaxed is $\Delta U = M\varepsilon_s t_s b_x$. The work per unit thickness needed to cause a migration of the edge dislocation from the bottom of the substrate to the interface is

$$\begin{aligned} W &= -\int_{r_0}^{t_s} F(z)\, dz = -\frac{G[b_x^2 + b_y^2 + (1-\nu)b_z^2]}{4\pi(1-\nu)} \int_{r_0}^{t_s} \left(\frac{1}{z} - \frac{1}{t_s + t_f - z} \right) dz \\ &= -\frac{G[b_x^2 + b_y^2 + (1-\nu)b_z^2]}{4\pi\ (1-\nu)} \ln \frac{t_s t_f}{r_0(t_s + t_f)}. \end{aligned} \tag{W20.13}$$

where r_0 is a cutoff parameter of atomic dimensions at which macroscopic elasticity theory breaks down. The bottom of the substrate is at $z = 0$. Equating W and ΔU

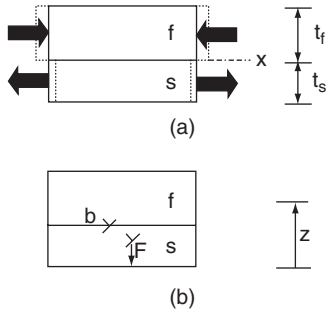

Figure W20.1. (*a*) Film on a substrate subjected to stresses due to lattice mismatch for the case $a_f > a_s$; (*b*) an edge dislocation migrates from a surface to the interface. [From L. B. Freund and W. D. Nix, *Appl. Phys. Lett.*, **69**, 173 (1996). Copyright 1996, American Institute of Physics.]

results in the formula

$$\varepsilon_m = \frac{b_x^2 + b_y^2 + (1-\nu)b_z^2}{8\pi(1+\nu)b_x t_c} \ln \frac{t_c}{r_0}, \tag{W20.14}$$

where a reduced critical thickness is defined by $1/t_c \equiv 1/t_{fc} + 1/t_{sc}$. Equation (W20.14) expresses ε_m in terms of t_c, but this may be inverted numerically to give t_c in terms of ε_m. Note that if the substrate is thick, t_c gives the film thickness t_{fc} directly.

Typical experimental data for Ge_xSi_{1-x} films deposited on a thick Si substrate[†] give the critical thickness as approximately 1000, 100, 10, and 1 nm for $x = 0.1$, 0.3, 0.5, and 1.0, respectively.

W20.3 Ionic Solutions

The description of an ionic solution involves specifying the ionic densities, $n_\pm(\mathbf{r})$, the solvent density, $n_s(\mathbf{r})$, and the potential, $\phi(\mathbf{r})$, as functions of the spatial position $\mathbf{r}$. The presence of a solid such as a metal or semiconductor is likely to introduce spatial inhomogeneities in these quantities. Far from the solid one may expect these variables to reach the limiting values $n_\pm^\infty$, n_s^∞, and ϕ^∞, respectively. It is convenient to take $\phi^\infty \equiv 0$. If the ionic charges are z_+e and $-z_-e$, then bulk neutrality requires that $z_+n_+^\infty = z_-n_-^\infty$. Near the solid deviations from neutrality occur and electric fields are present. In this section the relationship between these quantities is studied.

It is convenient to use a variational principle to derive these equations[‡]. At $T = 0$ K the familiar Poisson equation may be derived from the energy functional:

$$U = \int d\mathbf{r}\, u = \int d\mathbf{r} \left[-\frac{\epsilon}{2}(\nabla\phi)^2 + z_+ e n_+ \phi - z_- e n_- \phi \right]. \tag{W20.15}$$

By using the Euler–Lagrange equation

$$\nabla \cdot \left(\frac{\partial u}{\partial \nabla \phi} \right) = \frac{\partial u}{\partial \phi}, \tag{W20.16}$$

one obtains

$$\nabla^2 \phi = -\frac{e}{\epsilon}(z_+ n_+ - z_- n_-), \tag{W20.17}$$

where ϵ is the electric permittivity of the solvent.

For $T > 0$ K one constructs a quantity analogous to the Helmholtz free energy:

$$F = \int d\mathbf{r}\, f = U - TS, \tag{W20.18}$$

[†] J. C. Bean et al., *J. Vac. Sci. Technol.*, **A2**, 436 (1984).

[‡] The approach is similar to that of I. Borukhov, D. Andelman, and H. Orland, *Phys. Rev. Lett.*, **79**, 435 (1997).

where S is the entropy, defined in terms of an entropy density, s,

$$S = \int d\mathbf{r}\, s. \tag{W20.19}$$

To obtain s imagine partitioning the volume of the solvent into boxes of size V. The number of ions of a given type in a box is $N_\pm = n_\pm V$, and the number of solvent molecules is $N_s = n_s V$. Idealize the situation by imagining that each particle (positive ion, negative ion, or solvent molecule) occupies the same volume. Let N be the number of sites available in volume V. Then $N = N_+ + N_- + N_s$. The number of ways of distributing the particles among the N sites is $W = N!/(N_+!\,N_-!\,N_s!)$. The entropy for the box is given by $S = sV = k_B \ln(W)$. Use of Stirling's approximation results in the expression

$$S = -k_B \int d\mathbf{r} \left(n_+ \ln \frac{n_+}{n} + n_- \ln \frac{n_-}{n} + n_s \ln \frac{n_s}{n} \right), \tag{W20.20}$$

where $n = N/V$. The total numbers of positive and negative ions are fixed. One varies F subject to these constraints

$$\delta \left(F - \mu_+ \int d\mathbf{r}\, n_+(\mathbf{r}) - \mu_- \int d\mathbf{r}\, n_-(\mathbf{r}) \right) = 0, \tag{W20.21}$$

where the chemical potentials $\mu_\pm$ are Lagrange multipliers. Variation with respect to $n_\pm$ and ϕ leads to the Poisson equation, as before, and

$$n_\pm(\mathbf{r}) = (n - n_+(\mathbf{r}) - n_-(\mathbf{r})) \exp[-\beta(\pm z_\pm e\phi(\mathbf{r}) - \mu_\pm)], \tag{W20.22}$$

where $\beta = 1/k_B T$ and use has been made of the fact that $n_s + n_+ + n_- = n$. Evaluating this far from the solid, where $\phi(\mathbf{r}) \to 0$, yields

$$\mu_\pm = k_B T \ln \frac{n_\pm^\infty}{n - n_\pm^\infty - n_\pm^\infty (z_\pm / z_\mp)}. \tag{W20.23}$$

The Poisson equation becomes

$$\nabla^2 \phi = -\frac{ne}{\epsilon} \frac{z_+ n_+^\infty \exp(-\beta z_+ e\phi) - z_- n_-^\infty \exp(\beta z_- e\phi)}{n_s^\infty + n_+^\infty \exp(-\beta z_+ e\phi) + n_-^\infty \exp(\beta z_- e\phi)}. \tag{W20.24}$$

At high charge densities on an interface the right-hand side saturates at a maximum value. Thus, if $\mp\beta z_\pm e\phi \gg 1$,

$$\nabla^2 \phi = \mp \frac{ne}{\epsilon} z_\pm. \tag{W20.25}$$

In the limit where $n_\pm \ll n$ the denominator simplifies and Eq. (W20.24) reduces to what is called the *Poisson–Boltzmann equation*:

$$\nabla^2 \phi = -\frac{e}{\epsilon} [z_+ n_+^\infty \exp(-\beta z_+ e\phi) - z_- n_-^\infty \exp(\beta z_- e\phi)]. \tag{W20.26}$$

In the limit where $|\beta z_{\pm} e\phi| \ll 1$, this reduces further to the *Debye–Hückel* equation:

$$\nabla^2\phi = \frac{1}{\lambda_D^2}\phi, \tag{W20.27}$$

where λ_D is the Debye screening length, given by

$$\frac{1}{\lambda_D^2} = \frac{e^2}{\epsilon k_B T}(z_+^2 n_+^\infty + z_-^2 n_-^\infty). \tag{W20.28}$$

In this case the potential will fall off exponentially with distance as $\phi(z) \propto \exp(-z/\lambda_D)$. The distance λ_D determines the range over which the charge neutrality condition is violated and an electric field exists.

Returning to Eq. (W20.24), in the one-dimensional case, let the solid occupy the half-space $z < 0$. One may obtain a first integral by multiplying through by $d\phi/dz$ and integrating from 0 to ∞:

$$\frac{\beta\epsilon}{2}\left(\frac{d\phi}{dz}\right)^2\bigg|_{z=0} = n \ln \frac{n_s^\infty + n_+^\infty \exp(-\beta z_+ e\phi_0) + n_-^\infty \exp(\beta z_- e\phi_0)}{n_s^\infty + n_+^\infty + n_-^\infty} \tag{W20.29}$$

where ϕ_0 is the solid-surface potential. The quantity $d\phi/dz$ is the negative of the electric field and is related to the charge density on the surface through the boundary condition that D_z is continuous. This is also partly determined by solving the Poisson equation inside the solid and linking the two solutions across the surface. The interface between a semiconductor and an ionic solution is considered in Section W20.4.

W20.4 Solid–Electrolyte Interface

Having considered both the semiconductor and the ionic solution in isolation, we are now in a position to combine them and to study their interface. Some aspects of solid–ionic solution systems have been encountered in Section W12.4 in the discussion of corrosion and oxidation, and in Section 19.11 concerning anodization. To be somewhat general, imagine that both a metal surface and a semiconductor surface are involved (Fig. W20.2). In thermal equilibrium the chemical potential of the electrons is constant throughout the system. Furthermore, there has to be net charge neutrality. Consider what happens when an electrochemical reaction occurs involving an exchange of electrons with the solids. An example is the reduction–oxidation reaction (redox couple) $H_2 \rightleftharpoons 2H^+ + 2e^-$. In the forward direction the reaction is the oxidation of H_2. In the backward direction it is the reduction of H^+. Each species is characterized by its own unique chemical potential in the electrolyte. To dissociate and ionize the H_2 molecule, energy must be supplied equal to the difference in energy between the two species. For the moment, any complications caused by the realignment of the solvation shell of solvent molecules are ignored. The solvation shell consists of those water molecules in the immediate vicinity of the ion whose dipole moments are somewhat aligned by the electric field of the ion.

More generally, consider the redox couple between two hypothetical ionic species labeled A_1 and A_2, of ionic charges $z_1 e$ and $z_2 e$, respectively:

$$n_1 A_1 \rightleftharpoons n_2 A_2 + n e^-. \tag{W20.30}$$

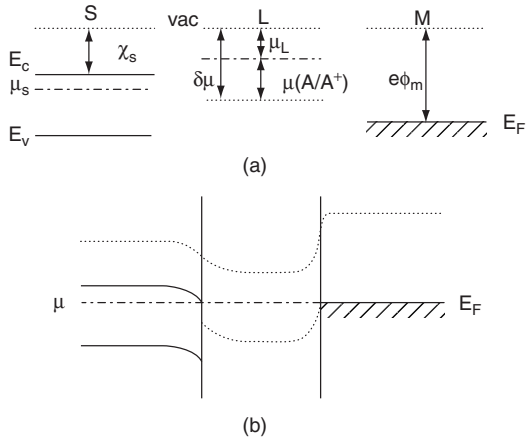

Figure W20.2. Band bending and equalization of Fermi levels in the semiconductor–electrolyte–metal system: (*a*) semiconductor (S), electrolyte (L), and metal (M) in isolation, sharing a common vacuum level; (*b*) band-bending and electrostatic-potential profile when the materials are brought in contact.

The chemical potentials obey the relation

$$n_1(\mu_1 + z_1 e\phi) = n_2(\mu_2 + z_2 e\phi) + n(\mu - e\phi), \tag{W20.31}$$

where the energy shift due to the local electrostatic potential is included. The chemical potentials in solution are given in terms of the activities by the Nernst equation:

$$\mu_i \equiv -ez_i\varepsilon_i = -ez_i\varepsilon_i^0 + k_B T \ln a_i, \tag{W20.32}$$

where ε_i^0 and a_i are the standard electrode potentials and activities of species A_i, respectively. To a first approximation the activities are often set equal to the fractional concentrations, c_i:

$$\mu_i \approx -ez_i\varepsilon_i^0 + k_B T \ln c_i. \tag{W20.33}$$

Charge conservation gives

$$z_1 n_1 = z_2 n_2 - n. \tag{W20.34}$$

Therefore, μ is a sensitive function of the ionic concentrations:

$$\begin{aligned} \mu &= \frac{n_1\mu_1 - n_2\mu_2}{n} \\ &= e\varepsilon - \frac{k_B T}{n} \ln \frac{(c_2)^{n_2}}{(c_1)^{n_1}}. \end{aligned} \tag{W20.35}$$

Here

$$\varepsilon = \frac{n_2 z_2 \varepsilon_2^0 - n_1 z_1 \varepsilon_1^0}{n} \tag{W20.36}$$

is called the *standard redox potential* of the couple. At any given point in the electrolyte the redox reaction is driven backwards or forwards, allowing concentrations of species 1 and 2 to adjust so as to maintain the chemical potentials at constant levels.

In the description above, the energy of reduction of a positive ion (i.e., the energy needed to add an electron to the ion) equals the energy of oxidation (i.e., the energy needed to remove an electron from an atom to create a positive ion). However, when the response of the solvent is included, these energies no longer coincide. The solvent molecules adjust themselves so as to minimize the Coulomb energy of the system. Since charge-exchange reactions alter the net ionic charge, there is a solvent shift of the energy levels. Thermal fluctuations in the solvent cause the energy levels to fluctuate in time. Whenever the energy balance condition is satisfied, a resonant charge exchange process can occur.

The convention is to take the hydrogen couple $H_2 \rightleftharpoons 2H^+ + 2e^-$ as the reference level by which to measure the *redox potentials* (the standard electrode potentials) of other redox couples. Typical couples are presented in Table W20.1 along with their standard redox potentials. The entries are arranged according to how good a reducing agent the atoms are. Thus Li is a strong reducing agent (i.e., it readily donates electrons to a solid). F_2 is a strong oxidizing agent, readily accepting electrons from a solid.

Equation (W20.35) must be modified for use in describing the solid–electrolyte interface. The problem arises because of the arbitrariness of the choice of the hydrogen couple in defining the zero of the standard redox potential. For use in describing the solid–electrolyte interface, both chemical potentials must be referred to the same reference level (e.g., vacuum). It is therefore necessary to find the difference between the standard redox potentials and the energies relative to vacuum, $\delta\mu$ (see Fig. W20.2). Thus Eq. (W20.35) should be replaced by

$$\mu = e\varepsilon + \delta\mu - \frac{k_B T}{n} \ln \frac{(c_2)^{n_2}}{(c_1)^{n_1}}. \tag{W20.37}$$

The value of the offset energy $\delta\mu$ is obtained by looking at the Gibbs free-energy changes (i.e., $\Delta_r G^o$) for a series of reactions (Morrison, 1980) and comparing the result to the value quoted for the standard redox potential:

$Ag^+(g) + e^-$	$= Ag(g)$	-7.57 eV
$Ag(g)$	$= Ag(s)$	-2.95 eV
$Ag^+(aq)$	$= Ag^+(g)$	$+5.00$ eV
$Ag^+(aq) + e^-$	$= Ag(s)$	-5.52 eV

The first line corresponds to the free-space ionization of a silver atom. The second line introduces the cohesive energy of silver. The third line utilizes a calculated value for the solvation energy of a silver ion in water. The solvation energy is the difference in electrostatic energy of an ion of charge +e at the center of a spherical cavity in the water and the electrostatic energy of the ion in free space:

$$U = -\frac{e^2}{8\pi\epsilon_0 a}\left(1 - \frac{1}{\epsilon_r}\right). \tag{W20.38}$$

Here a is the metallic radius of Ag^+ (0.145 nm) and $\epsilon_r(0) = 80$ is the static dielectric constant for H_2O at $T = 27°C$. The value of the standard redox potential for the reaction $Ag^+(aq) + e^- = Ag(s)$ (Table W20.1) is 0.800 eV. Thus $\delta\mu = -5.52 + 0.80 = -4.72$ eV. However, this value must be regarded as being only approximate. It disregards the solvation energy of the electron and underestimates the radius of the solvation shell. Typically, values for $\delta\mu$ in the range -4.5 to -4.8 eV are employed in the literature.

Electrons in an isolated semiconductor will, in general, have a chemical potential which is different from that of an electron in an electrolyte. This is illustrated in Fig. W20.2. The upper half of the diagram shows the semiconductor (S), electrolyte (L), and metal (M) isolated from each other, sharing a common vacuum level. Note that the chemical potential of an electron in the electrolyte, μ_L, is determined by subtracting the chemical potential for the redox couple, $\mu(A/A^+)$ [given by Eq. (W20.37)], from the offset energy $\delta\mu$, as in Fig. W20.2.

When the two are brought into contact, as in the lower half of Fig. W20.2, there will be a charge transfer and the chemical potentials will equilibrate. This will cause band bending in the semiconductor in much the same way that it was caused in the p-n junction. At the two interfaces there is not charge neutrality and electric fields exist due to the dipole double layers.

W20.5 Multilayer Materials

One rather simple use of multilayers is to fabricate optical materials with interpolated gross physical characteristics. For example, one could achieve an interpolated index of refraction n by alternating sufficiently thin layers of indices n_1 and n_2. The linear interpolation formula, $n = (1 - f)n_1 + fn_2$, where f is the fraction of space occupied by material 2, would only give a crude approximation to n and is not physically

TABLE W20.1 Standard Redox Potential Energies at $T = 25°C$

Redox Couple	ε (V)
$Li = Li^+ + e^-$	3.045
$Rb = Rb^+ + e^-$	2.925
$K = K^+ + e^-$	2.924
$Cs = Cs^+ + e^-$	2.923
$Na = Na^+ + e^-$	2.711
$Mn = Mn^{2+} + 2e^-$	1.029
$Zn = Zn^{2+} + 2e^-$	0.763
$Cu = Cu^{2+} + 2e^-$	0.34
$Pb = Pb^{2+} + 2e^-$	0.126
$H_2 = 2H^+ + 2e^-$	0.000
$Cu^+ = Cu^{2+} + e^-$	−0.153
$Fe^{2+} = Fe^{3+} + e^-$	−0.770
$Ag = Ag^+ + e^-$	−0.800
$2Br^- = Br_2 + 2e^-$	−1.065
$2Cl^- = Cl_2 + 2e^-$	−1.358
$2F^- = F_2 + 2e^-$	−2.870

motivated. A better interpolation could be obtained by recalling that $n_i = \sqrt{\epsilon_{r_i}}$ and making use of the Clausius–Mossotti formula, Eq. (8.40). That formula showed that the ratio $(n^2 - 1)/(n^2 + 2)$ may be expressed as a linear combination of polarizability contributions from each of the materials present in a composite medium. Thus an appropriate interpolation formula would be

$$\frac{n^2 - 1}{n^2 + 2} = (1 - f)\frac{n_1^2 - 1}{n_1^2 + 2} + f\frac{n_2^2 - 1}{n_2^2 + 2}. \tag{W20.39}$$

The design is valid provided that the length scale of the periodicity is small compared with the wavelength of light.

The linear interpolation formula $\kappa = (1 - f)\kappa_1 + f\kappa_2$ could be used to fabricate materials with interpolated thermal conductivities. However, this is only approximate, since the interface region between two media often has different physical properties from either medium, including its own thermal resistance due to phonon scattering.

As another example of linear interpolation, suppose that there are two physical properties, denoted by n and p, that one would like to obtain. Assume that there are three materials, with values (n_1, n_2, n_3) and (p_1, p_2, p_3), respectively. Construct the multilayer by taking lengths (a_1, a_2, a_3) such that the superlattice has periodicity

$$a_1 + a_2 + a_3 = D. \tag{W20.40}$$

Then, assuming simple additivity of the properties, one has

$$a_1 n_1 + a_2 n_2 + a_3 n_3 = Dn, \tag{W20.41a}$$

$$a_1 p_1 + a_2 p_2 + a_3 p_3 = Dp. \tag{W20.41b}$$

These three linear equations may be solved for the lengths a_1, a_2, and a_3. One finds that

$$\frac{a_1}{D} = \frac{1}{\Delta}[(n_2 p_3 - p_2 n_3) + (p_2 - p_3)n + (n_2 - n_3)p], \tag{W20.42a}$$

$$\frac{a_2}{D} = \frac{1}{\Delta}[(n_3 p_1 - p_3 n_1) + (p_3 - p_1)n + (n_3 - n_1)p], \tag{W20.42b}$$

$$\frac{a_3}{D} = \frac{1}{\Delta}[(n_1 p_2 - p_1 n_2) + (p_1 - p_2)n + (n_1 - n_2)p], \tag{W20.42c}$$

where

$$\Delta = n_2 p_3 + n_3 p_1 + n_1 p_2 - p_2 n_3 - p_3 n_1 - p_1 n_2. \tag{W20.43}$$

The extension to a higher number of variables is obvious.

W20.6 Second-Harmonic Generation in Phase-Matched Multilayers

Nonlinear polarization is introduced in Section 8.9 and discussed further in Section 18.6. For efficient second-harmonic generation one needs two things: a material with a large nonlinear electrical susceptibility and birefringence. The latter is needed so that

phase matching between the primary beam at frequency ω and the secondary beam at frequency 2ω can be obtained over a long coherence length. The semiconductor GaAs has a large $\chi^{(2)}$ (240 pm/V) but is a cubic crystal, so is optically isotropic and not birefringent. By constructing a multilayer structure with interspersed thin layers of oxidized AlAs (Alox), artificial birefringence is obtained[†].

Here one uses the approximate additivity of the dielectric function for the TE mode of propagation:

$$\epsilon_{\mathrm{TE}} = (1 - f)\epsilon_{r_1} + f\epsilon_{r_2}. \tag{W20.44}$$

The TE mode of a waveguide has the electric field perpendicular to the direction of propagation, but the magnetic field need not be. Similarly, the approximate additivity of the inverse of the dielectric function for the TM mode of propagation yields

$$\frac{1}{\epsilon_{\mathrm{TM}}} = \frac{1 - f}{\epsilon_{r_1}} + \frac{f}{\epsilon_{r_2}}. \tag{W20.45}$$

The TM mode has a magnetic field perpendicular to the propagation direction. In Eqs. (W20.44) and (W20.45), ϵ_{r_1} and ϵ_{r_2} are the respective dielectric functions of the materials and f is the filling fraction. The respective indices of refraction for GaAs and Alox are $n_1 = \sqrt{\epsilon_{r_1}} = 3.6$ and $n_2 = \sqrt{\epsilon_{r_2}} = 1.6$. The net birefringence is determined by the difference in the indices of refraction for the TE and TM modes:

$$\Delta n = \sqrt{\epsilon_{\mathrm{TE}}} - \sqrt{\epsilon_{\mathrm{TM}}}. \tag{W20.46}$$

This, in turn, is a function of the filling fraction and may therefore be engineered to specifications.

The same concept may be used to the advantage of another nonlinear process, *difference frequency generation* (DFG). In this process, photons of frequencies ω_1 and ω_2 are mixed together to produce a photon of frequency $|\omega_1 - \omega_2|$.

W20.7 Organic Light-Emitting Diodes

Recently, a structure composed partly of stacked organic films was designed to act as a tunable three-color transparent organic light-emitting diode (TOLED). Since the additive primary colors are red, blue, and green, this device can function as a universal light-emitting diode. The structure is illustrated in Fig. W20.3. Electron injection into the upper organic layer is through the low work function Mg:Ag cathode. The transparent conductor indium tin oxide (ITO) serves as the anodes. The organic molecules used are 4,4′-bis[*N*-(1-napthyl)-*N*-phenylamino]biphenyl (α-NPD), which is a hole conductor, bis(8-hydroxy)quinaldine aluminum phenoxide ($\mathrm{Alq}_2'\mathrm{Oph}$), which fluoresces in the blue, and tris(8-hydroxyquinoline aluminum) (Alq_3), which is an electron conductor and fluoresces in the green. By doping Alq_3 with 3% 5,10,15,20-tetraphenyl-21*H*,23*H*-porphine (TPP), the fluorescent band is pulled down to the red. A layer of crystalline 3,4,9,10-perylenetetracarboxylic dianhydride (PTCDA) serves as a transparent hole conductor and shields the sensitive organic layer against ITO sputtering. One of the

[†] A. Fiory et al., *Nature*, **391**, 463 (1998).

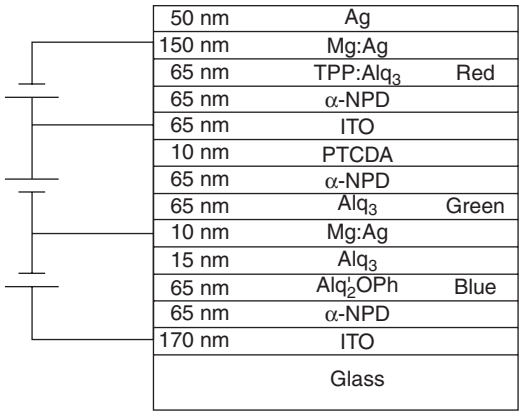

Figure W20.3. Three-color tunable organic light-emitting device. [Reprinted with permission from Z. Shen et al., *Science*, **276**, 2009 (1997). Copyright 1997, American Association for the Advancement of science.]

keys to success in fabricating this device is that amorphous and organic films tend not to be tied down by the need to satisfy lattice-matching constraints.

W20.8 Quasiperiodic Nonlinear Optical Crystals

A recent application of multilayer structures to the field of nonlinear optics involves the construction of a periodic superlattice. For example, to carry out second-harmonic generation efficiently, phase matching is required (i.e., the material must be able to simultaneously satisfy momentum and energy conservation). However, $\mathbf{k}(2\omega) - 2\mathbf{k}(\omega) = \mathbf{K}_{21} \neq 0$, in general. Similarly, for third-harmonic generation, $\mathbf{k}(3\omega) - 3\mathbf{k}(\omega) = \mathbf{K}_{31} \neq 0$. By constructing a superlattice with the periodicity $2\pi/K_{21}$ or $2\pi/K_{31}$, the index of refraction will possess this periodicity and will be able to supply the missing wave vector. The strength of the scattering amplitude will involve the Fourier component of the index of refraction at that wave vector. This scheme has been applied to such nonlinear crystals as $LiNbO_3$.

It is also possible to construct a quasiperiodic lattice (one-dimensional quasicrystal) which can supply K_{21} and K_{31} simultaneously. It is assumed that these wave vectors are such that K_{31}/K_{21} is not a rational number. Such a structure can be based on the Fibonacci sequence of layers ABAABABAABAAB.... Such a crystal using $LiTaO_3$ has been built[†]. In that scheme the A and B layers each had a pair of antiparallel ferroelectric domains. The thicknesses of the domains were L_{A1} and L_{A2} in layer A and L_{B1} and L_{B2} in layer B. Let $L_A = L_{A1} + L_{A2}$ and $L_B = L_{B1} + L_{B2}$ and assume that $L_{A1} = L_{B1} = L$. Let $L_{A2} = L(1 + \eta)$ and $L_{B2} = L(1 - \eta\tau)$, with $\tau = (1 + \sqrt{5})/2$ and η a small number. Let $D = \tau L_A + L_B$ be a characteristic distance. Then the vectors $G_{m,n}$ serve as quasiperiodic reciprocal-lattice vectors

$$G_{m,n} = \frac{2\pi}{D}(m + n\tau). \tag{W20.47}$$

[†] S. Zhu et al., *Science*, **278**, 843(1997).

There exist a set of numbers (m_1, n_1) that make $G_{m_1,n_1} \approx K_{21}$ and another pair (m_2, n_2) that make $G_{m_2,n_2} \approx K_{31}$. Thus both K_{21} and K_{31} are provided by the structure. In the reference cited above, the values used for the structural parameters were $L = 10.7$ μm and $\eta = 0.23$.

W20.9 Graphite Intercalated Compounds

Graphite consists of graphene layers of sp^2-bonded carbon rings arranged in the stacking sequence ABAB... and separated by 0.335 nm, which is substantially larger than the nearest-neighbor distance of 0.142 nm. The in-plane lattice constant of the hexagonal sheet is 0.246 nm. The layers are only weakly bound together by van der Waals forces. It is possible to insert foreign atoms and molecules in the interlayer region to form graphite intercalated compounds (GICs). It is found that the atoms intercalate in well-defined stoichiometric ratios, forming compounds such as KC_{24}. In one type of arrangement one layer of intercalate is followed by n graphene layers, as illustrated in Fig. W20.4*a*. This is called an *n-stage GIC*. For example, KC_{24} can exist as a two-stage compound $KC_{12\times2}$ or a three-stage compound $KC_{8\times3}$. Values of n up to 8, or higher, are not uncommon. In other compounds there may be several intercalate layers, followed by n graphene layers. In still other situations the intercalates may form islands arranged in an array interspersed in the graphite structure (the Daumas–Herold domain structure). This is illustrated in Fig. W20.4*b*.

The distance between successive intercalate layers, d_c, depends on the degree of staging. Different forms of ordering are found in the GICs. The intercalated layers could either be commensurate or incommensurate with the host lattice. The graphene layers could either maintain the ABAB.... stacking sequence or adopt some other sequence, such as AB/BA/AB/BA/... (where a slash denotes an intercalated layer). The intercalate could exist as an ordered two-dimensional crystal, a disordered glass, or even a liquid.

The intercalated atoms and molecules may act as either donors or acceptors. In either case, carriers are injected into the π bands of the graphene sheet. Typical donors are the alkali metals, which form GICs such as LiC_6, LiC_{12}, LiC_{18}, KC_8, KC_{24}, ... ,

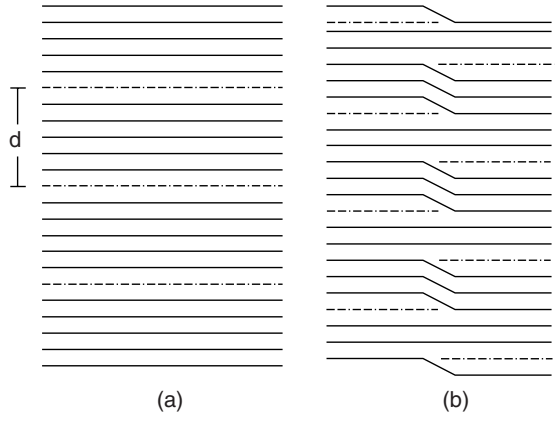

Figure W20.4. Graphite intercalated compounds: (*a*) $n = 5$ stage compound; (*b*) island intercalation.

KC_{72}, RbC_8, RbC_{24} or CsC_8, and CsC_{24}. Acceptor compounds are $C_{10}HNO_3$, $C_{14}Br$, or $C_{16}AsF_5$. Note the convention of placing the chemical symbol for the donors to the left of the carbon and the symbol for acceptors to the right.

Staging results from the interplay of various microscopic forces. Charge transfer is brought about by the difference in chemical potentials between the graphite and the intercalate. This, by itself, lowers the energy of the system. The Coulomb interaction between the layers, partially screened by the mobile carriers in the graphite, is important in establishing the staging. Elastic interactions are also involved, since the layer spacing of the host lattice is altered to accommodate the intercalated layer. One of the early attempts[†] at describing the system theoretically involved the introduction of the model internal energy:

$$\frac{U}{N_0} = t\sum_i \sigma_i - \frac{u}{2}\sum_i \sigma_i^2 + \frac{1}{2}{\sum_{ij}}' V_{ij}\sigma_i\sigma_j, \tag{W20.48}$$

where N_0 is the number of intercalation sites in a layer and σ_i is the fractional occupancy of the ith layer, a number between 0 and 1. The first two terms represent the interaction of the intercalate with the host, and the bonding of the intercalate to form a two-dimensional solid, respectively. The third term describes the screened Coulomb energy and is positive. The parameters V_{ij} are taken to be of the form $V_{ij} = (V/2)|z_{ij}|^{-\alpha}$, where z_{ij} is the interplanar distance. This form is suggested by making a Thomas–Fermi analysis of the screening for large n. The quantities t, u, V, and $\alpha(\approx 5)$ parametrize the theory.

The entropy for a given layer is determined by partitioning $N_0\sigma_i$ intercalate atoms among N_0 sites. Since there are $W_i = N_0!/[(N_0\sigma_i)!(N_0 - N_0\sigma_i)!]$ ways of doing this, the layer entropy is, by Stirling's approximation,

$$S_i = k_B \ln W_i = -k_B N_0[\sigma_i \ln \sigma_i + (1-\sigma_i)\ln(1-\sigma_i)]. \tag{W20.49}$$

The Helmholtz free energy for the system is

$$\frac{F}{N_0} = t\sum_i \sigma_i - \frac{u}{2}\sum_i \sigma_i^2 + \frac{1}{2}{\sum_{ij}}' V_{ij}\sigma_i\sigma_j + k_BT\sum_i[\sigma_i \ln \sigma_i + (1-\sigma_i)\ln(1-\sigma_i)]. \tag{W20.50}$$

Only the layers with nonzero σ_i contribute to F. The chemical potential for the ith layer is given by

$$\mu_i = \frac{1}{N_0}\frac{\partial F}{\partial \sigma_i} = t - u\sigma_i + {\sum_j}' V_{ij}\sigma_j + k_BT\left[\ln \sigma_i - \ln(1-\sigma_i)\right]. \tag{W20.51}$$

Setting all the chemical potentials equal to μ leads to the set of coupled equations

$$\sigma_i = \frac{1}{1 + e^{\beta(t - u\sigma_i + {\sum_j}' V_{ij}\sigma_j - \mu)}}. \tag{W20.52}$$

[†] S. A. Safran, Stage ordering in intercalation compounds, H. Ehrenreich and D. Turnbull, eds., *Solid State Physics*, Vol. 40, Academic Press, San Diego, Calif., 1987, p. 183.

For a given set of staging occupancies it is possible to obtain $\mu(T)$, F, and the other thermodynamic variables.

Further refinements in the theory have evolved over the years. Interest in GICs stems largely from the fact that their electrical conductivity is high and may be varied in a controlled way by changing the stoichiometry.

Graphite fluorides $(CF)_n$ have been used as cathodes in lithium batteries. By itself, $(CF)_n$ is a poor electrical conductor, so it is often combined with a good electrical conductor such as graphite. The anode is made of lithium. Such lithium batteries have high specific energy (360 W·h/kg) and a high voltage (3 V). The material $(CF)_n$ is a stage 1 compound with every C atom bonded to a fluorine. The layers alternate in the sequence CFCFCF. . . . The lattice constants are $a = 0.257$ nm and $c = 0.585$ nm.

Other GICs that may potentially be used as cathodes have intercalant anions such as PF_6^-, AsF_6^-, and SbF_6^-. The obstacle to their use is the lack of a suitable electrolyte. Superconductivity is also observed in GICs (see Chapter W16).

REFERENCES

Critical Thickness

Freund, L B., and W. D. Nix, *Appl. Phys. Lett.*, **69**, 173 (1996).

Ionic Solutions

Borukhov, I., D. Andelman, and H. Orland, *Phys. Rev. Letters.*, **79**, 435 (1997).

Solid-Electrolyte Interface

Morrison, S. R., *Electrochemistry at Semiconductor and Oxide Metal Electrodes*, Plenum Press, New York, 1980.

Second-Harmonic Generation in Phase-Matched Multilayers

Fiory, A., et al., *Nature*, **391**, 463 (1998).

Organic Light-Emitting Diodes

Shen, Z., et al., *Science*, **276**, 2009 (1997).

Quasi-periodic Nonlinear Optical Crystals

Zhu, S., et al., *Science*, **278**, 843 (1997).

Graphite Intercalated Compounds

Zabel, H., and S. A. Solin, eds., *Graphite Intercalation Compounds*, Springer-Verlag, New York, 1990.

PROBLEM

W20.1 Consider the case of a thin film deposited on a thick substrate ($t_f \ll t_s$).

(a) Show that the resulting strains in the substrate and film are $\epsilon_s \approx 0$ and $\epsilon_f \approx (a_{s0} - a_{f0})/a_{f0}$, respectively, where a_{s0} and a_{f0} are the stress-free lattice constants of the substrate and film.

(b) Show that the strain in the film can be relieved completely if the misfit dislocations at the film/substrate interface are, on the average, separated by a distance $d = a_{s0}/|\epsilon_m|$, where ϵ_m is the misfit strain defined by Eq. (W20.8).